

## ARTICLE

# Molecular Dissection of Isolated Disease Features in Mosaic Neurofibromatosis Type 1

Ophélie Maertens, Sofie De Schepper, Jo Vandesompele, Hilde Brems, Ine Heyns, Sandra Janssens, Frank Speleman, Eric Legius, and Ludwine Messiaen

Elucidation of the biological framework underlying the development of neurofibromatosis type 1 (NF1)-related symptoms has proved to be difficult. Complicating factors include the large size of the *NF1* gene, the presence of several *NF1* pseudogenes, the complex interactions between cell types, and the *NF1*-haploinsufficient state of all cells in the body. Here, we investigate three patients with distinct NF1-associated clinical manifestations (neurofibromas only, pigmentary changes only, and association of both symptoms). For each patient, various tissues and cell types were tested with comprehensive and quantitative assays capable of detecting low-percentage *NF1* mutations. This approach confirmed the biallelic *NF1* inactivation in Schwann cells in neurofibromas and, for the first time, demonstrated biallelic *NF1* inactivation in melanocytes in NF1-related café-au-lait macules. Interestingly, both disease features arise even within a background of predominantly *NF1* wild-type cells. Together, the data provide molecular evidence that (1) the distinct clinical picture of the patients is due to mosaicism for the *NF1* mutation and (2) the mosaic phenotype reflects the embryonic timing and, accordingly, the neural crest-derived cell type involved in the somatic *NF1* mutation. The study of the affected cell types provides important insight into developmental concepts underlying particular NF1-related disease features and opens avenues for improved diagnosis and genetic counseling of individuals with mosaic NF1.

Neurofibromatosis type 1 (NF1 [MIM 162200]) is a common autosomal dominant disorder caused by alterations in the *NF1* gene. The *NF1*-encoded protein, neurofibromin, functions as a negative regulator of Ras-mediated signaling.<sup>1–3</sup> The primary clinical features of NF1 are café-au-lait macules (CALMs), freckling, and benign peripheral nerve sheath tumors or neurofibromas.<sup>4</sup> Patients with NF1 also have a predisposition to develop a wide spectrum of other symptoms, illustrating the critical function of neurofibromin in a variety of tissues and cell types. The biological context underlying the development of many NF1-related symptoms and complications, however, remains incompletely understood.

Mosaic NF1 is caused by a postzygotic *NF1* lesion<sup>5–7</sup> and can present as mild generalized disease, segmental disease, or gonadal mosaicism.<sup>8</sup> Revertant mosaicism, as reported to be caused by a postzygotic back mutation in some disorders,<sup>9</sup> has not yet been described in cases of NF1. The mosaic phenotype most probably reflects the timing of the somatic mutation and some of the tissues affected by it. Since segmental NF1 is characterized by the regionally limited distribution of NF1 disease signs, it provides the opportunity to study cell populations differing only with regard to the mutation(s) giving rise to mosaicism. Determining when and in what cell types inactivation of the *NF1* gene occurs is critical for understanding the basic pathology of NF1-related symptoms.

In this study, we investigated one patient mildly affected with NF1 and two patients with segmental NF1. The three patients had different clinical manifestations—that is, neurofibromas only, pigmentary changes only, and a combination of both neurofibromas and pigmentary changes. To elucidate the involvement of particular cell types and mutational mechanisms in the respective phenotypes, we investigated various tissues and cell types from every patient with mosaic NF1 with quantitative assays capable of detecting low-percentage *NF1* mutations.

## Material and Methods

### Patient Material

Three patients with distinct NF1-associated clinical manifestations were included in the study.

**Neurofibromas only.**—Patient SNF1-1 is a 46-year-old woman who has several small (1–4 mm) cutaneous neurofibromas clustered within a limited body region on her trunk and neck. At a given time, 35–40 neurofibromas were present. Several tumors have been removed during different sessions, and three were available for this study. She also underwent surgery for an intestinal ganglioneuroma (S100 and neurofilament positive; c-Kit negative). Careful examination did not reveal freckling or localized hyperpigmentation. Only three hyperpigmented spots smaller than 2 cm were present. She had no Lisch nodules, no learning disabilities, and no other signs of NF1 except for a glomus tumor at the distal phalanx of the right middle finger. Her height is 164 cm, and there was no clinical evidence of macrocrania. Her par-

From the Center for Medical Genetics (O.M.; J.V.; S.J.; F.S.; L.M.) and Department of Dermatology (S.D.S.), Ghent University Hospital, Ghent, Belgium; Center of Human Genetics, Catholic University Leuven, Leuven, Belgium (H.B.; I.H.; E.L.); and Department of Genetics, University of Alabama at Birmingham, Birmingham (L.M.)

Received February 27, 2007; accepted for publication April 26, 2007; electronically published June 20, 2007.

Address for correspondence and reprints: Dr. Ludwine Messiaen, Medical Genomics Laboratory, University of Alabama at Birmingham, Kaul Human Genetics Building, Suite 330, 720 20th Street S, Birmingham, AL 35294-0024. E-mail: [lmessiaen@genetics.uab.edu](mailto:lmessiaen@genetics.uab.edu)  
*Am. J. Hum. Genet.* 2007;81:243–251. © 2007 by The American Society of Human Genetics. All rights reserved. 0002-9297/2007/8102-0006\$15.00  
DOI: 10.1086/519562

ents and her two sons (aged 20 and 23 years) don't show any NF1-related symptoms. Peripheral blood from the patient and her sons, as well as the patient's buccal smears, hair roots, urine, Schwann cells, and fibroblasts cultured from three neurofibromas, were available for analysis.

**Pigmentary defects only.**—Patient SNF1-2 is a 23-year-old man presenting with several CALMs within a background of hyperpigmented skin involving his entire right leg, hip, and lower back (fig. 1A). Inguinal freckling was present in the affected segment. No hyperpigmentation or CALMs were revealed outside the described area. Careful examination of his entire body did not reveal any neurofibromas. Ophthalmological examination findings were negative for Lisch nodules. His height is 182 cm, and his head circumference is 58 cm. He has no learning disabilities; currently, he is a high school student. He does not have children, and his parents do not show any NF1-related symptoms. Peripheral blood, buccal smears, hair roots, and urine sediment cells were available for investigation, as were fibroblasts and melanocytes cultured from normal skin, CALM, and the hyperpigmented area.

**Pigmentary defects and neurofibromas.**—Patient SNF1-3 is a 15-year-old girl with more than six CALMs scattered over her body and several small cutaneous and subcutaneous neurofibromas located on her right hand within an overlying CALM (fig. 1B). CALMs (>1.5 cm) not occurring within regions of hyperpigmented skin are located on her right lower back (two), right arm (one on the front [fig. 1B] and one on the back), left wrist (one), left thigh (one), left ankle (one), left gluteal region (one), right calf (one), right thigh (two), and right groin (two). Total-body nuclear magnetic resonance imaging (MRI) revealed a putative neurofibroma on her left shoulder. Physical examination did not reveal skinfold freckling or any other signs of NF1. Her height is 163.5 cm, and her head circumference is 55 cm. She does not have learning disabilities, and her parents do not show any NF1-related symptoms. Peripheral blood, buccal smears, hair roots,

and urine sediment cells, together with Schwann cells and fibroblasts derived from one subcutaneous neurofibroma and fibroblasts and melanocytes derived from three CALMs (on her right hand, left thigh, and right lower back) and from normal skin (right buttock), were available for analysis. MRI of the patient's right hand revealed a subcutaneous nodule with a few smaller surrounding subcutaneous satellite lesions. Histopathologically, the lesions were determined to be neurofibromas by the absence of mitotic activity and the mixture of elongated spindle-shaped Schwann cells and fibroblasts in a background of wavy collagenous fibers. This diagnosis was confirmed by immunohistochemistry (S100 positivity in the majority of spindle-shaped cells).

### Cell Culture

**Skin biopsy.**—A sample of normally pigmented and/or hyperpigmented skin was taken using 5-mm punch biopsy excision. To separate the epidermal layer (with melanocytes anchored to the basal membrane) from the underlying dermis (with fibroblasts), skin biopsy samples were incubated overnight at 4°C in dispase II (Boehringer Mannheim). Primary epidermal melanocyte cultures from the skin biopsy samples were established as described elsewhere.<sup>10</sup> In brief, melanocytes were cultured in Ham's F10 medium (Gibco, Invitrogen) supplemented with 2.5% fetal calf serum (FCS), 1% Ultrosor, 5 ng/ml basic fibroblast growth factor, 10 ng/ml endothelin-1, 0.33 nM cholera toxin, 0.033 mM isobutyl-methyl-xanthine, 5.3 nM 12-O-tetradecanoyl phorbol-13-acetate, and 20 ng/ml stem cell factor (SCF). Dermal fibroblasts were grown in Dulbecco's modified Eagle medium (Gibco, Invitrogen) supplemented with 10% FCS.

**Neurofibroma.**—Culture conditions for neurofibroma-derived Schwann cells and fibroblasts were as described elsewhere.<sup>11,12</sup> The presence of forskolin (F+) in the Schwann cell medium promotes proliferation of cells bearing only the first hit (*NF1*<sup>+/−</sup>, SC F+).

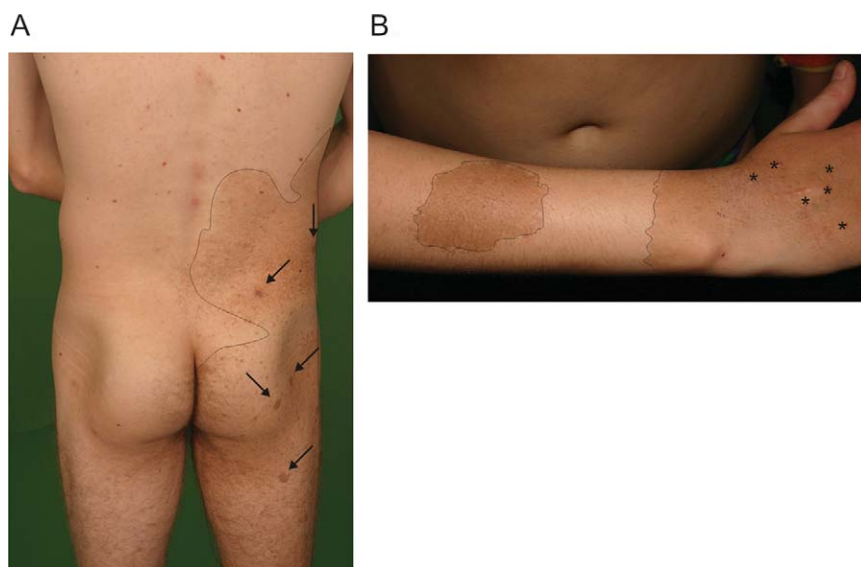


**Figure 1.** Illustration of clinical subtypes of patients with mosaic NF1. *A*, Patient SNF1-2 presented with several CALMs (arrows) within a pigmented background involving the entire right leg, hip, and lower back (outlined). *B*, Patient SNF1-3 presented with more than six CALMs (one outlined on the left) scattered over the body and several small neurofibromas (asterisks) located on the right hand within an overlying CALM (outlined on the right).

Replacement of proliferation medium by serum-free N<sub>2</sub> medium and, subsequently, by proliferation medium without forskolin (F<sup>−</sup>) promotes proliferation of cells containing both hits (*NF1*<sup>−/−</sup>). To estimate the purity of Schwann cell and fibroblast cultures derived from the neurofibroma of patient SNF1-3, immunofluorescence staining with rabbit S100 primary antibody (Dako) was performed as described elsewhere.<sup>13</sup> For one SC F<sup>−</sup> culture (patient SNF1-1, neurofibroma 3), Schwann cells were separated from contaminating fibroblasts by the use of p75 (nerve growth factor receptor)–coupled Magnetic Cell Sorting Microbeads (Miltenyi Biotec), which magnetically label the Schwann cell target population. Subsequent growth of recovered cells in Schwann cell medium resulted in a highly pure Schwann cell culture (>95%, estimated by S100 staining).

### NF1 Mutation Screening

*NF1* mutation analysis (GenBank reference sequence NM\_000267) was performed essentially as described elsewhere.<sup>14</sup> In brief, genomic DNA (gDNA) was extracted from melanocyte cultures with the QiaAmp procedure (Qiagen) and from all other cell cultures with the Puregene procedure (Gentra). Cultures were treated with puromycin (200 µg/ml for 4–6 h) before RNA extraction (RNeasy kit [Qiagen]). The entire *NF1* cDNA was sequenced using the ABI3730XL genetic analyzer (Applied Biosystems). All mutations found at the cDNA level were confirmed in gDNA by cycle sequencing. Multiplex ligation-dependent probe amplification (MLPA) analysis was performed using the SALSA NF1 area kit (MRC Holland), in accordance with the manufacturer's instructions, to detect deletions.

### Fine Mapping NF1 Deletion Breakpoints

The genomic deletions detected by MLPA analysis were evaluated in further detail. The location of the *NF1* microdeletion breakpoints was determined by specifically amplifying and sequencing paralogous sequence variants (PSVs) in the low copy repeats (LCRs) flanking the *NF1* microdeletion region.<sup>15</sup> By scoring the relative intensity of both nucleotides of the PSV, the location of the breakpoint was determined to be centromeric (higher relative intensity of the nucleotide specific to the telomeric LCR) or telomeric (higher relative intensity of the nucleotide specific to the centromeric LCR) of the PSV investigated.

### Loss of Heterozygosity in NF1 Region

Loss of heterozygosity (LOH) in the *NF1* gene region was evaluated by genotyping two microsatellite markers telomeric of (3' NF1-3 and 3' NF1-1)<sup>16</sup> and four within the *NF1* gene (*Alu*, IVS27AC33.1, IVS38GT53.0, and IVS27TG24.8).<sup>17–20</sup> gDNA from paired melanocyte/Schwann cell and lymphocyte cultures from the same patient was investigated by touchdown PCR for the microsatellite markers (PCR program starting at 62°C, gradually reduced [1°C/cycle] to 50°C for an additional 25 cycles) and was subsequently analyzed on the ABI3130XL genetic analyzer (Applied Biosystems) with GeneMapper software version 3.7 (Applied Biosystems). To determine the extent of LOH in different samples from patient SNF1-3, additional SNPs proximal (*rs6505129*, *rs6505165*, and *rs8071580*) and distal (*rs9904537* and *rs753750*) to the *NF1* microdeletion region were evaluated as described elsewhere.<sup>21</sup> LOH for a SNP was scored when the average ratio (SNP nucleotide:control nucleotide) of the two alleles in the tested tissue fell outside the 95% CI of the ratios observed in control

blood DNA of the same patient and when the average ratios in tested tissue versus control blood were at least 20% different. The mechanism underlying LOH (deletion vs. mitotic recombination) was evaluated by semiquantitative PCR, which took advantage of the amplification of *NF1* exon 22 (103 bp) together with the corresponding fragment of its pseudogene located on chromosome 15 (107 bp), as described elsewhere.<sup>21</sup>

### Cloning NF1 Point Mutations

To determine whether both *NF1* mutations detected in SC F<sup>−</sup> cultures derived from the neurofibromas of patient SNF1-1 resided on different alleles, cloning experiments were performed. For neurofibroma 1 (*NF1* c.2041C→T and c.1655T→G), a fragment containing both alterations and an additional SNP in exon 13 (*rs2285892*) was amplified (516 bp), cloned in the pCR2.1-TOPO Vector (Invitrogen), and sequenced. For neurofibroma 2 (*NF1* c.2041C→T and c.603\_621delinsC), a fragment containing the deletion and a SNP in exon 5 (*rs1801052*) was amplified (286 bp), cloned, and sequenced. Since *rs1801052* and *rs2285892* are in complete linkage disequilibrium, information on the genotype of the SNP in exon 13 linked with the first hit (cloning experiment neurofibroma 1) and information on the genotype of the SNP in exon 5 linked with the second hit (cloning experiment neurofibroma 2) provide information regarding whether both mutations reside on the same (exon 5/exon13: A/G or G/A) or different (exon5/exon13: A/A or G/G) haplotypes.

### Quantification of NF1 Mutations

**Real-time quantitative PCR.**—To detect low-percentage mosaicism for *NF1* point mutations against a background of normal and pseudogene alleles, a nested real-time quantitative PCR (qPCR) assay was developed.<sup>22</sup> In brief, the region spanning the *NF1* point mutation was amplified (primer sequences available on request), and equimolar dilutions of cloned PCR fragments (wild-type and mutant alleles) were used to generate standard curves of 5 orders of magnitude. For actual quantification, allele-specific 3' locked nucleic acid primers (Eurogentec) were used. Since both somatic *NF1* point mutations appeared to be present in several *NF1* pseudogenes, samples were first amplified with *NF1* specific primer pairs and were diluted prior to nested real-time qPCR. Real-time qPCR reactions were performed on an iCycler iQ instrument (Bio-Rad). In each experiment, duplicates of a standard dilution series of specific PCR fragments for each allele variant (wild-type and mutant) and triplicates of 10 ng DNA of unknown samples (different tissues from patient with mosaic NF1 under study and non-NF1 control sample) were amplified in a 15-µl reaction containing 1 × SYBR Green I Master Mix (Eurogentec) and 250 nM of allele-specific primers. The thermal profile consisted of 1 cycle at 95°C for 10 min followed by 40 cycles at 95°C for 15 s and at 61°C or 63°C for 1 min. Each experiment was performed twice, and data acquisition and automated analysis was done by the iCycler iQ software version 3.1 (Bio-Rad). The relative number of molecules of each allele was determined by interpolating the threshold cycle values of the unknown samples to each standard curve, followed by the determination of the fraction of mutant alleles (number of mutant molecules divided by the sum of the number of wild-type and mutant molecules).

**FISH analysis.**—Submicroscopic *NF1* deletions were scored using dual-color FISH<sup>23</sup> with PAC clones 22 (RP5-926B9; 5' NF1) and 13 (RP5-1002G3; 3' NF1).<sup>16</sup> To investigate mosaicism, at least 400

**Table 1. Overview of *NF1* Mutations Revealed by Routine Mutation-Detection Techniques and Real-Time qPCR in Different Tissues Derived from Segmental Patient SNF1-1, Presenting with Neurofibromas Only, and from Two Sons**

Patient and Sample <sup>a</sup>	c.2041C→T (p.R681X)		Second Hit
	Routine	qPCR <sup>b</sup>	
SNF1-1:			
Neurofibroma 1:			
SC F—	+	41.4% ± 6.4%	c.1655T→G (p.L552R)
Fibroblasts	—	8.4% ± .5%	—
Neurofibroma 2:			
SC F—	+	47.4% ± 8.6%	c.603_621delinsC
Fibroblasts	—	19.4% ± 5.5%	—
Neurofibroma 3:			
SC F—	—	6.7% ± 1.0%	—
Fibroblasts	—	—	—
Blood	—	3.7% ± .4%	—
Buccal smear	—	—	—
Urine	—	—	—
Hair	—	1.8% ± .3%	—
Child 1:			
Blood	—	—	—
Child 2:			
Blood	—	—	—

NOTE.—+ = Mutation detectable; — = mutation not detectable.

<sup>a</sup> SC F— = Schwann cells grown without forskolin.

<sup>b</sup> Percentage of mutant allele ± SEM determined by real-time qPCR.

interphase nuclei were evaluated. By analysis of control samples derived from patients not affected with *NF1*, the sensitivity of the assay was estimated at 1% for lymphocytes and 7% for fibroblasts.

## Results

### Neurofibromas Only (Patient SNF1-1)

*NF1* mutation screening of selectively cultured Schwann cells (SC F—) revealed an identical mutation (c.2041C→T [p.R681X]) in two different neurofibromas. In addition, two tumor-specific alterations (c.1655T→G [p.L552R] and c.603\_621delinsC) were detected. Cloning experiments demonstrated that both *NF1* mutations (common and tumor specific) resided on different alleles. Quantification of mutant transcripts in the presence of the wild-type form was tested by mixing an excess ( $5 \times 10^5$  molecules) of wild-type allele with a 5-point 10-fold dilution series of the mutant form ( $5 \times 10^5$ —50 molecules). As a control, a standard curve containing only the mutant transcript was used. Ideally, both series should result in overlapping amplification plots. We observed, however, that, at low levels of mutant transcript (<2,500 molecules), the presence of the wild-type transcript ( $5 \times 10^5$  molecules) significantly impaired accurate quantification of the low-abundance mutant transcript. Therefore, the sensitivity of the quantitative assay is estimated at 1/200. Real-time qPCR demonstrated the presence of the first hit (mutant allele percentage ± SEM) in Epstein Barr virus-transformed white blood cells ( $3.7\% \pm .4\%$ ), hair follicles ( $1.8\% \pm 0.3\%$ ), fibroblasts derived from both neurofibromas ( $8.4\% \pm 0.5\%$

and  $19.4\% \pm 5.5\%$ ), and selectively cultured Schwann cells from a third, smaller neurofibroma ( $6.7\% \pm 1.0\%$ ). Findings from buccal smears, urine sediment cells, and fibroblasts derived from the third neurofibroma were negative or below the detection limit, as were findings from blood from both children of the patient and the control sample (table 1).

### Pigmentary Defects Only (Patient SNF1-2)

Combined *NF1* cDNA sequencing and MLPA analysis revealed an *NF1* microdeletion exclusively present in the melanocytes derived from CALMs and the background hyperpigmentation area. A second alteration (c.1226\_1227del) was detected only in the melanocytes of the CALM. Further characterization of the microdeletion revealed an atypical deletion, with the proximal breakpoint residing within the centromeric LCR flanking the *NF1* gene and the distal breakpoint located centromeric of the telomeric LCR flanking the *NF1* gene before *JJAZ1* exon 7 (maximum size of the deletion 1.30 Mb). FISH analysis of skin fibroblasts (CALM and hyperpigmented and unaffected skin) with *NF1*-specific probes did not show evidence of low-level mosaicism when the detection limit of 7% was taken into account (table 2). FISH analysis of blood lymphocytes revealed a slightly increased number of nuclei with evidence of *NF1* microdeletion (8 [2%] nuclei with one *NF1* locus detected by two-color FISH in a total of 400 evaluated nuclei) (table 2), as compared with the non-*NF1* control lymphocyte sample (0.01;  $P = .050$ ; binomial test).

**Table 2. Overview of *NF1* Mutations Revealed by Routine Mutation-Detection Techniques and FISH Analysis in Different Tissues Derived from Segmental Patient SNF1-2, Presenting with Pigmentary Defects Only**

Sample	<i>NF1</i> Microdeletion		Second Hit
	Routine	FISH <sup>a</sup>	
CALM:			
Melanocytes	+	ND	c.1226_1227del
Fibroblasts	—	<7%	—
Hyperpigmentation:			
Melanocytes	+	ND	—
Fibroblasts	—	<7%	—
Unaffected skin:			
Melanocytes	—	ND	—
Fibroblasts	—	<7%	—
Blood	—	2%	—
Buccal smear	—	ND	—
Urine	—	ND	—
Hair	—	ND	—

NOTE.—+ = Mutation detectable; — = mutation not detectable.

<sup>a</sup> Percentage of 400 interphase nuclei with *NF1* microdeletion determined by FISH analysis. ND = no data available.



**Table 3. Overview of *NF1* Mutations Revealed by Routine Mutation-Detection Techniques and Quantitative Assays (FISH and Real-Time qPCR) in Different Tissues Derived from Mosaic Patient SNF1-3, Presenting with Neurofibromas and Pigmentary Defects, and from Family Members**

Patient and Sample <sup>a</sup>	S100 <sup>b</sup>	<i>NF1</i>		c.2325+1G→A	
		Microdeletion		Routine	qPCR <sup>d</sup>
		Routine	FISH <sup>c</sup>		
SNF1-3:					
Neurofibroma (right hand):					
SC F−	>95%	+	ND	+	88.8% ± 8.7%
SC F+	>95%	+	ND	+	67.2% ± 9.5%
Fibroblasts	~10%	−	ND	+	12.3% ± 1.8%
CALM (right hand):					
Melanocytes	NA	+	ND	+	97.1% ± 8.2%
Fibroblasts	NA	−	<7%	−	2.0% ± .3%
CALM (left thigh):					
Melanocytes	NA	+	ND	+	71.8% ± 5.5%
Fibroblasts	NA	−	<7%	−	—
CALM (right lower back):					
Melanocytes	NA	+	ND	+	54.9% ± 9.1%
Fibroblasts	NA	−	<7%	−	—
Normal skin (right buttock):					
Melanocytes	NA	−	ND	−	—
Fibroblasts	NA	−	<7%	−	—
Blood	NA	−	4%	−	—
Buccal smear	NA	−	ND	−	—
Urine	NA	−	ND	−	—
Hair	NA	−	ND	−	ND
Mother:					
Blood	NA	−	ND	−	—
Father:					
Blood	NA	−	ND	−	—
Brother:					
Blood	NA	−	ND	−	—
Sister:					
Blood	NA	−	ND	−	—

NOTE.—+ = Mutation detectable; – = mutation not detectable. ND = no data available.

<sup>a</sup> Schwann cells (SC) grown with (F+) or without (F–) forskolin.

<sup>b</sup> Percentage of cells positive for S100 immunostaining. NA = not applicable.

<sup>c</sup> Percentage of 400 interphase nuclei with *NF1* microdeletion determined by FISH analysis.

<sup>d</sup> Percentage mutant allele ± SEM determined by real-time qPCR.

#### *Pigmentary Defects and Neurofibromas (Patient SNF1-3)*

Analysis of neurofibroma-derived Schwann cells (SC F+ and SC F–) and melanocytes derived from both the CALM on the right hand and two CALMs remote from that zone revealed an identical *NF1* mutation (c.2325+1G→A) leading to out-of-frame skipping of exon 14, as well as a deletion of the other *NF1* allele. For all samples, the proximal deletion breakpoint resided between *rs6505129* (chromosome 17 reference position 24777972 [National Center for Biotechnology Information build 36.2]) and *rs6505165* (position 25598975), whereas the distal deletion breakpoint resided between the most distal PSV in the telomeric *NF1* LCR (position 27439522) and *rs9904537* (position 27579216) (minimum/maximum size of deletion 1.84 Mb/2.80 Mb). To test the influence of excess wild-type transcript on detection of the mutant transcript (c.2325+1G→A), a 5-point 10-fold dilution series of the

mutant form ( $5 \times 10^5$ –50 molecules) was mixed with excess wild-type ( $5 \times 10^5$  molecules). Equal amounts of water (instead of wild-type transcript) were added to a second series of dilutions. Comparison of both amplification plots revealed that, at low levels of mutant transcript (<1,250 molecules), the presence of the wild-type transcript significantly impaired accurate quantification of the low-abundance mutated transcript. Therefore, the sensitivity of the quantitative assay is estimated at 1/400. Real-time qPCR demonstrated the presence of the intragenic *NF1* mutation (mutant allele percentage ± SEM) in fibroblasts derived from both the neurofibroma (12.3% ± 1.8%) and the CALM on the right hand (2.0% ± 0.3%). Findings from melanocytes and fibroblasts derived from normal skin, fibroblasts derived from both CALMs on the left thigh and right lower back, peripheral blood, buccal smear, urine sediment cells, and the control sample were negative. As

expected, the mutation could not be detected in peripheral blood from the parents and siblings of the patient (table 3). FISH analysis of skin fibroblasts (CALM and unaffected skin) with *NF1*-specific probes did not show evidence of low-level mosaicism when the detection limit of 7% was taken into account (table 3). FISH analysis of blood lymphocytes revealed a significantly increased number of nuclei with evidence of *NF1* microdeletion (15/400 [4%]) (table 3) as compared with the non-*NF1* control lymphocyte sample (0.01;  $P = .000017$ ; binomial test). Immunofluorescence staining revealed S100-positive cells in the SC F- (>95%), SC F+ (>95%), and fibroblast (~10%) cultures derived from the neurofibroma.

## Discussion

In this study, three patients with mosaic *NF1* with different clinical manifestations were investigated at the molecular level to provide insight into the cell types and mutational mechanisms involved in the development of particular *NF1*-related disease features.

### *Neurofibromas Only (Patient SNF1-1)*

In selectively cultured Schwann cells (SC F-) derived from two neurofibromas, an identical *NF1* mutation, in addition to two tumor-specific alterations on the other allele, was detected, clearly confirming the tumor-initiating properties of Schwann cells in neurofibroma development.<sup>11,24,25</sup> Quantitative mutation screening of fibroblasts derived from both neurofibromas revealed only low percentages of mutant (first-hit) allele ( $8.4\% \pm 0.5\%$  and  $19.4\% \pm 5.5\%$ ), which is undetectable by conventional mutation-detection techniques (i.e., PCR *NF1* exon 13 and subsequent sequencing), and might reflect contamination of the fibroblast culture with Schwann cells (see patient SNF1-3). Similarly, Shultz et al.<sup>26</sup> could not demonstrate any *NF1* mutation in neurofibroma-derived fibroblasts from a patient with segmental *NF1* by use of the protein truncation test, enzymatic mutation detection, and FISH. Remarkably, only a limited amount of mutant allele ( $6.7\% \pm 1.0\%$ ) was detected in selectively cultured Schwann cells (purity estimated at >95% by S100 staining) from a third, smaller tumor, further illustrating the high abundance of *NF1*<sup>+/+</sup> cells in the tumor microenvironment. A growing body of experimental evidence supports the idea that *NF1* haploinsufficiency in the tumor environment promotes (plexiform) neurofibroma formation in mice.<sup>27-31</sup> Haploinsufficient mast cells, for example, have been shown to be hypermigratory and to have increased survival and proliferation potential in response to SCF secreted by *Nf1*<sup>-/-</sup> Schwann cells.<sup>28,30</sup> Whether the abundance of *NF1* wild-type cells in (dermal) neurofibromas from patients with segmental *NF1* reflects a slightly different pathogenesis or, alternatively, is associated with the small size of these patients' tumors (heterozygous neighboring cells may promote tumor growth more effi-

ciently than wild-type neighboring cells) remains an important and intriguing question.

### *Pigmentary Defects Only (Patient SNF1-2)*

Combined *NF1* cDNA sequencing and MLPA analysis revealed an *NF1* microdeletion exclusively present in melanocytes derived from affected skin of patient SNF1-2 (table 2). Although a high frequency of mosaic *NF1* microdeletions are caused by somatic recombination of the *JJAZ1* gene,<sup>32</sup> the current *NF1* lesion does not represent a typical type II deletion. A second alteration (c.1226\_1227del) was present only in melanocytes derived from the CALM but not in the hyperpigmented background area. Previously, Eisenbarth et al.<sup>33</sup> did not detect somatic *NF1* inactivation in melanocytes cultured from 10 CALMs of patients with classic *NF1*. The discrepancy with the current data can probably be explained by different melanocyte culture conditions and by the fact that, in the previous report, the cells were analyzed only for LOH at the *NF1* locus, whereas we performed a comprehensive *NF1* mutation screening. Available evidence suggests that paracrine cytokines interacting between epidermal melanocytes and nonmelanocytic cells in the skin play a central role in epidermal hyperpigmentation (reviewed by Imokawa<sup>34</sup>). Although the etiopathogenesis of *NF1*-related pigmentary lesions remains largely unknown, it has been postulated that the mechanism of epidermal hyperpigmentation and mast cell infiltration in *NF1* CALMs might be associated with increased secretion of cytokines such as SCF and hepatocyte growth factor by dermal fibroblasts.<sup>35</sup> Along the same line, De Schepper et al.<sup>36</sup> reported increased levels of soluble SCF in fibroblast supernatant from *NF1* CALM but, importantly, also in *NF1* normal skin compared with control individuals. In other words, paracrine networks are at play in the *NF1* skin but are not sufficient for CALM development. Here, we demonstrate that biallelic *NF1* inactivation in the melanocytes may be required for CALM formation, whereas, even in the haploinsufficient state, the *NF1* gene presumably has an effect on general skin pigmentation. Recently, a significant increase in melanocyte density was demonstrated in *NF1* CALM skin compared with *NF1* normal skin, control normal skin, and control CALM skin.<sup>36</sup> These *NF1* CALM melanocytes also display a higher melanin content and melanogenesis.<sup>37</sup> In light of our current findings, it is tempting to speculate that biallelic *NF1* inactivation in melanocytes might be the underlying molecular mechanism for the distinct properties of these *NF1*-related pigmentary lesions. In a next step, it will be essential to determine the dysregulating consequences of neurofibromin loss and *NF1* haploinsufficiency on signaling pathways in melanocytes. Previous studies on segmental pigmentary lesions revealed *NF1* mutations in 9% and 18% of fibroblasts<sup>6,7</sup> and in 20% of keratinocytes<sup>7</sup> cultured from CALMs. In this study, FISH analysis of fibroblasts derived from the hyperpigmentary and CALM skin lesions of pa-

tient SNF1-2 was unable to show an *NF1* microdeletion (table 2). Therefore, we speculate that pigmentary lesions can arise within an environment consisting of predominantly *NF1* wild-type cells.

Interestingly, inactivation of the *NF1* gene has been demonstrated elsewhere in sporadic malignant melanoma cell lines<sup>38,39</sup> and recently also in an early-disease-stage melanoma arising in a 15-year-old patient with NF1.<sup>40</sup> Although a definite association between malignant melanoma and NF1 has not yet been established, these data suggest that the *NF1* gene acts as a tumor suppressor gene in melanocytes in benign CALMs as well as in malignant melanomas.

#### *Pigmentary Defects and Neurofibromas (Patient SNF1-3)*

In patient SNF1-3, an *NF1* mutation (c.2325+1G→A) was revealed in neurofibroma-derived Schwann cells, as well as in melanocytes derived from both the CALM on the right hand and two CALMs remote from that zone. Moreover, all samples showed deletion of the other *NF1* allele (1.84 Mb–2.80 Mb). Unfortunately, insufficient material was available to further pinpoint the deletion breakpoints by high-resolution techniques. Since melanocytes and Schwann cells can arise from a bipotent glial-melanocyte precursor,<sup>41</sup> it is possible that one or both *NF1* mutations occurred in a common neural crest precursor. The clinical observation of neurofibromas arising within an overlying CALM might be compatible with this hypothesis. In other words, inactivation of the wild-type *NF1* allele at the heterozygous *NF1* locus in an early developmental stage (e.g., neural crest precursor giving rise to bipotent glial-melanocytic cells<sup>41</sup>) might be responsible for the segmental involvement of epidermis (melanocyte) and several nerve branches (Schwann cell). Alternatively, a melanocytic precursor bearing both hits might have migrated to the right hand area and then locally reversed to glia through a neural crest–derived glial-melanocytic progenitor.<sup>41</sup> Unexpectedly, the *NF1* point mutation was also detected in neurofibroma-derived fibroblasts (culture passage 2), albeit at a significantly lower frequency (12.3% ± 1.8%). Immunofluorescence staining demonstrated that the latter observation most probably can be explained by the presence of S100-positive cells (Schwann cells and/or melanocytes) in the fibroblast cultures. Quantitative *NF1* mutation screening in blood revealed a low percentage of mosaicism for the *NF1* microdeletion only (table 3). This observation most probably implies that the *NF1* microdeletion represents the first hit. Quantitative mutation screening also revealed a low percentage of the first hit in blood from patients SNF1-1 and SNF1-2 (tables 1 and 2). Obviously, these observations raise questions about the developmental timing of the mutational event and also the embryological origin of the mutation-bearing cells in the blood. Possibly, the respective first hits might have occurred in a multipotent stem cell giving rise to neural crest cells as well as hematopoietic cells. Alternatively,

neural crest stem cells might give rise to a small percentage of circulating blood cells. It is well established that different cutaneous neurofibromas from the same patient with NF1 bear different second hits (patient SNF1-1 and patients described elsewhere<sup>13</sup>). Moreover, these neurofibromas usually become apparent only during the 2nd decade of life.<sup>4</sup> Strikingly, both *NF1* inactivating events are the same in the melanocytes derived from the CALMs on the right hand, the left thigh, and the right lower back. This finding is particularly intriguing, given the typical congenital appearance of many NF1 CALM lesions. It remains to be further explored whether the early presentation of pigmentary NF1 signs could be attributed to biallelic *NF1* inactivation in melanocytic precursors (melanoblasts) during embryonic development. Melanoblasts migrate in mice from the neural crest dorsolaterally and enter the skin where they proliferate clonally and finally differentiate into mature skin melanocytes.<sup>42,43</sup> One might assume that neurofibromin loss in melanoblasts will result in enhanced proliferation and, hence, increased melanocyte density<sup>36</sup> in NF1-related CALM lesions. It will be essential to molecularly dissect more CALM lesions derived from different areas of the body and to determine the (presumably different) second hit in NF1 clinical features arising only later in life.

The molecular data obtained from all patients with mosaic NF1 described in this article undeniably indicate that the percentage of the *NF1* mutation in non–neural crest–derived cells is often so low that it would be missed by routine *NF1* screening. This implies that an accurate diagnosis for mosaic NF1 can be established only by comprehensive screening of those cells responsible for the phenotypic NF1-related features—that is, Schwann cells in neurofibromas and/or melanocytes in pigmentary lesions. Additionally, screening the relevant cell type in the patient with mosaic NF1 can provide a molecular marker useful in the prenatal and presymptomatic diagnostic setting. This new insight will incontestably facilitate the diagnosis and counseling of individuals with mosaic NF1. Moreover, the molecular approaches described in this article might prove beneficial in those 5% of patients fulfilling the NF1 National Institutes of Health clinical criteria but in whom no constitutional *NF1* mutation can be revealed in blood (e.g., patient SNF1-3). Also, for this particular patient group, comprehensive screening of NF1 phenotype-related cell types will facilitate clinical diagnosis and further genetic follow-up.

In conclusion, we provide—for the first time, to our knowledge—molecular evidence that different NF1 mosaic phenotypes result from a postzygotic *NF1* mutation in neural crest–derived cell types. Whereas *NF1* deficiency in Schwann cells is essential for neurofibroma development, biallelic *NF1* inactivation in melanocytes seems to trigger NF1-related CALM development. In our opinion, the clinical mosaic phenotype points to cell types that are irrefutably affected by the somatic *NF1* mutation. These findings provide important insight into the developmen-

tal concepts underlying NF1-related disease features and open avenues for improved diagnosis and genetic counseling for individuals with mosaic NF1.

## Acknowledgments

We thank Martine De Mil for technical assistance with melanocyte culturing. This work is supported by Interuniversity Attraction Poles grant P5/25 from the Federal Office for Scientific, Technical and Cultural Affairs, Belgium (2002–2006), by a Concerted Action Grant from UGent, and by a Concerted Action Grant from KULeuven. E.L. is a part-time clinical researcher, S.D.S. is a predoctoral researcher, and J.V. is a postdoctoral researcher with the Fonds voor Wetenschappelijk Onderzoek Vlaanderen. This work is also supported by Belgische Federatie tegen Kanker grant SCIE2003-33 (to E.L.). We thank the Wilderman family for their donation (to L.M.) to help support NF1 research for children with CALMs only. Beta-heretulin for Schwann cell culture was provided by Genentech, San Francisco.

## Web Resources

The accession number and URLs for data presented herein are as follows:

GenBank, <http://www.ncbi.nlm.gov/Genbank> (for NF1 [reference sequence NM\_000267])

Online Mendelian Inheritance in Man (OMIM), <http://www.ncbi.nlm.nih.gov/Omim/> (for NF1)

## References

- Xu GF, Lin B, Tanaka K, Dunn D, Wood D, Gesteland R, White R, Weiss R, Tamanoi F (1990) The catalytic domain of the neurofibromatosis type 1 gene product stimulates ras GTPase and complements ira mutants of *S. cerevisiae*. *Cell* 63:835–841
- Martin GA, Viskochil D, Bollag G, McCabe PC, Crosier WJ, Haubruck H, Conroy L, Clark R, O'Connell P, Cawthon RM, et al (1990) The GAP-related domain of the neurofibromatosis type 1 gene product interacts with ras p21. *Cell* 63:843–849
- Ballester R, Marchuk D, Boguski M, Saulino A, Letcher R, Wigler M, Collins F (1990) The NF1 locus encodes a protein functionally related to mammalian GAP and yeast IRA proteins. *Cell* 63:851–859
- Riccardi VM (1992) Neurofibromatosis: phenotype, natural history and pathogenesis. John Hopkins University Press, Baltimore and London
- Vandenbroucke I, van Doorn R, Callens T, Cobben JM, Starink TM, Messiaen L (2004) Genetic and clinical mosaicism in a patient with neurofibromatosis type 1. *Hum Genet* 114:284–290
- Tinschert S, Naumann I, Stegmann E, Buske A, Kaufmann D, Thiel G, Jenne DE (2000) Segmental neurofibromatosis is caused by somatic mutation of the neurofibromatosis type 1 (NF1) gene. *Eur J Hum Genet* 8:455–459
- Consoli C, Moss C, Green S, Balderson D, Cooper DN, Upadhyaya M (2005) Gonosomal mosaicism for a nonsense mutation (R1947X) in the NF1 gene in segmental neurofibromatosis type 1. *J Invest Dermatol* 125:463–466
- Ruggieri M, Huson SM (2001) The clinical and diagnostic implications of mosaicism in the neurofibromatoses. *Neurology* 56:1433–1443
- Youssefian H, Pyeritz RE (2002) Mechanisms and consequences of somatic mosaicism in humans. *Nat Rev Genet* 3:748–758
- Naeyaert JM, Eller M, Gordon PR, Park HY, Gilchrist BA (1991) Pigment content of cultured human melanocytes does not correlate with tyrosinase message level. *Br J Dermatol* 125:297–303
- Serra E, Rosenbaum T, Winner U, Aledo R, Ars E, Estivill X, Lenard HG, Lazaro C (2000) Schwann cells harbor the somatic NF1 mutation in neurofibromas: evidence of two different Schwann cell subpopulations. *Hum Mol Genet* 9:3055–3064
- Rosenbaum T, Rosenbaum C, Winner U, Muller HW, Lenard HG, Hanemann CO (2000) Long-term culture and characterization of human neurofibroma-derived Schwann cells. *J Neurosci Res* 61:524–532
- Maertens O, Brems H, Vandesompele J, De Raedt T, Heyns I, Rosenbaum T, De Schepper S, De Paepe A, Mortier G, Janssens S, et al (2006) Comprehensive NF1 screening on cultured Schwann cells from neurofibromas. *Hum Mutat* 27:1030–1040
- Messiaen LM, Callens T, Mortier G, Beysen D, Vandenbroucke I, Van Roy N, Speleman F, De Paepe A (2000) Exhaustive mutation analysis of the NF1 gene allows identification of 95% of mutations and reveals a high frequency of unusual splicing defects. *Hum Mutat* 15:541–555
- De Raedt T, Stephens M, Heyns I, Brems H, Thijs D, Messiaen L, Stephens K, Lazaro C, Wimmer K, Kehrer-Sawatzki H, et al (2006) Conservation of hotspots for recombination in low-copy repeats associated with the NF1 microdeletion. *Nat Genet* 38:1419–1423
- Lopez-Correa C, Brems H, Lazaro C, Estivill X, Clementi M, Mason S, Rutkowski JL, Marynen P, Legius E (1999) Molecular studies in 20 submicroscopic neurofibromatosis type 1 gene deletions. *Hum Mutat* 14:387–393
- Xu GF, Nelson L, O'Connell P, White R (1991) An Alu polymorphism intragenic to the neurofibromatosis type 1 gene (NF1). *Nucleic Acids Res* 19:3764
- Lazaro C, Gaona A, Xu G, Weiss R, Estivill X (1993) A highly informative CA/GT repeat polymorphism in intron 38 of the human neurofibromatosis type 1 (NF1) gene. *Hum Genet* 92:429–430
- Lazaro C, Gaona A, Ravello A, Volpini V, Casals T, Fuentes JJ, Estivill X (1993) Novel alleles, hemizyosity and deletions at an Alu-repeat within the neurofibromatosis type 1 (NF1) gene. *Hum Mol Genet* 2:725–730
- Lazaro C, Gaona A, Estivill X (1994) Two CA/GT repeat polymorphisms in intron 27 of the human neurofibromatosis (NF1) gene. *Hum Genet* 93:351–352
- De Raedt T, Maertens O, Chmara M, Brems H, Heyns I, Sciort R, Majounie E, Upadhyaya M, De Schepper S, Speleman F, et al (2006) Somatic loss of wild type NF1 allele in neurofibromas: comparison of NF1 microdeletion and non-microdeletion patients. *Genes Chromosomes Cancer* 45:893–904
- Maertens O, Legius E, Speleman F, Messiaen L, Vandesompele J (2006) Real-time quantitative allele discrimination assay using 3' locked nucleic acid primers for detection of low-percentage mosaic mutations. *Anal Biochem* 359:144–146
- Van Roy N, Laureys G, Cheng NC, Willem P, Opdenakker G, Versteeg R, Speleman F (1994) 1;17 translocations and other chromosome 17 rearrangements in human primary neuroblastoma tumors and cell lines. *Genes Chromosomes Cancer* 10:103–114



24. Rutkowski JL, Wu K, Gutmann DH, Boyer PJ, Legius E (2000) Genetic and cellular defects contributing to benign tumor formation in neurofibromatosis type 1. *Hum Mol Genet* 9: 1059–1066
25. Kluwe L, Friedrich R, Mautner VF (1999) Loss of NF1 allele in Schwann cells but not in fibroblasts derived from an NF1-associated neurofibroma. *Genes Chromosomes Cancer* 24: 283–285
26. Schultz ES, Kaufmann D, Tinschert S, Schell H, von den Driesch P, Schuler G (2002) Segmental neurofibromatosis. *Dermatology* 204:296–297
27. Zhu Y, Ghosh P, Charnay P, Burns DK, Parada LF (2002) Neurofibromas in NF1: Schwann cell origin and role of tumor environment. *Science* 296:920–922
28. Yang FC, Ingram DA, Chen S, Hingtgen CM, Ratner N, Monk KR, Clegg T, White H, Mead L, Wenning MJ, et al (2003) Neurofibromin-deficient Schwann cells secrete a potent migratory stimulus for *Nf1* +/- mast cells. *J Clin Invest* 112: 1851–1861
29. Munchhof AM, Li F, White HA, Mead LE, Krier TR, Fenoglio A, Li X, Yuan J, Yang FC, Ingram DA (2006) Neurofibroma-associated growth factors activate a distinct signaling network to alter the function of neurofibromin-deficient endothelial cells. *Hum Mol Genet* 15:1858–1869
30. Ingram DA, Yang FC, Travers JB, Wenning MJ, Hiatt K, New S, Hood A, Shannon K, Williams DA, Clapp DW (2000) Genetic and biochemical evidence that haploinsufficiency of the *Nf1* tumor suppressor gene modulates melanocyte and mast cell fates in vivo. *J Exp Med* 191:181–188
31. Ingram DA, Hiatt K, King AJ, Fisher L, Shivakumar R, Derstine C, Wenning MJ, Diaz B, Travers JB, Hood A, et al (2001) Hyperactivation of p21(ras) and the hematopoietic-specific Rho GTPase, Rac2, cooperate to alter the proliferation of neurofibromin-deficient mast cells in vivo and in vitro. *J Exp Med* 194:57–69
32. Kehrer-Sawatzki H, Kluwe L, Sandig C, Kohn M, Wimmer K, Krammer U, Peyrl A, Jenne DE, Hansmann I, Mautner VF (2004) High frequency of mosaicism among patients with neurofibromatosis type 1 (NF1) with microdeletions caused by somatic recombination of the *JJAZ1* gene. *Am J Hum Genet* 75:410–423
33. Eisenbarth I, Assum G, Kaufmann D, Krone W (1997) Evidence for the presence of the second allele of the neurofibromatosis type 1 gene in melanocytes derived from cafe au lait macules of NF1 patients. *Biochem Biophys Res Commun* 237:138–141
34. Imokawa G (2004) Autocrine and paracrine regulation of melanocytes in human skin and in pigmentary disorders. *Pigment Cell Res* 17:96–110
35. Okazaki M, Yoshimura K, Suzuki Y, Uchida G, Kitano Y, Harii K, Imokawa G (2003) The mechanism of epidermal hyperpigmentation in cafe-au-lait macules of neurofibromatosis type 1 (von Recklinghausen's disease) may be associated with dermal fibroblast-derived stem cell factor and hepatocyte growth factor. *Br J Dermatol* 148:689–697
36. De Schepper S, Boucneau J, Vander Haeghen Y, Messiaen L, Naeyaert JM, Lambert J (2006) Café-au-lait spots in neurofibromatosis type 1 and in healthy control individuals: hyperpigmentation of a different kind? *Arch Dermatol Res* 297: 439–449
37. Kaufmann D, Wiandt S, Vesper J, Krone W (1991) Increased melanogenesis in cultured epidermal melanocytes from patients with neurofibromatosis 1 (NF 1). *Hum Genet* 87:144–150
38. Andersen LB, Fountain JW, Gutmann DH, Tarle SA, Glover TW, Dracopoli NC, Housman DE, Collins FS (1993) Mutations in the neurofibromatosis 1 gene in sporadic malignant melanoma cell lines. *Nat Genet* 3:118–121
39. Johnson MR, Look AT, DeClue JE, Valentine MB, Lowy DR (1993) Inactivation of the NF1 gene in human melanoma and neuroblastoma cell lines without impaired regulation of GTP·Ras. *Proc Natl Acad Sci USA* 90:5539–5543
40. Rubben A, Bausch B, Nikkels A (2006) Somatic deletion of the NF1 gene in a neurofibromatosis type 1-associated malignant melanoma demonstrated by digital PCR. *Mol Cancer* 5:36
41. Dupin E, Glavieux C, Vaigot P, Le Douarin NM (2000) Endothelin 3 induces the reversion of melanocytes to glia through a neural crest-derived glial-melanocytic progenitor. *Proc Natl Acad Sci USA* 97:7882–7887
42. Yoshida H, Kunisada T, Kusakabe M, Nishikawa S, Nishikawa SI (1996) Distinct stages of melanocyte differentiation revealed by analysis of nonuniform pigmentation patterns. *Development* 122:1207–1214
43. Wilkie AL, Jordan SA, Jackson IJ (2002) Neural crest progenitors of the melanocyte lineage: coat colour patterns revisited. *Development* 129:3349–3357